



**HAL**  
open science

# Molecular Agglomeration Index: Quantification of the Incidence of Asphaltene Molecular Agglomeration in Aged Asphalt Binders Through Rheological Measurements

Rodrigo Shigueiro Siroma, Mai Lan Nguyen, Pierre Hornych, Tristan Lorino, Yvong Hung, Aurélia Nicolai, Layella Ziyani, Emmanuel Chailleux

► **To cite this version:**

Rodrigo Shigueiro Siroma, Mai Lan Nguyen, Pierre Hornych, Tristan Lorino, Yvong Hung, et al.. Molecular Agglomeration Index: Quantification of the Incidence of Asphaltene Molecular Agglomeration in Aged Asphalt Binders Through Rheological Measurements. *Transportation Research Record*, 2022, 2676 (10), pp.89-103. 10.1177/03611981221088597. hal-04313050

**HAL Id: hal-04313050**

**<https://univ-eiffel.hal.science/hal-04313050>**

Submitted on 28 Nov 2023

**HAL** is a multi-disciplinary open access archive for the deposit and dissemination of scientific research documents, whether they are published or not. The documents may come from teaching and research institutions in France or abroad, or from public or private research centers.

L'archive ouverte pluridisciplinaire **HAL**, est destinée au dépôt et à la diffusion de documents scientifiques de niveau recherche, publiés ou non, émanant des établissements d'enseignement et de recherche français ou étrangers, des laboratoires publics ou privés.

1 **Molecular Agglomeration Index (MAI): Quantification of the Incidence of Asphaltene**  
2 **Molecular Agglomeration in Aged Asphalt Binders Through Rheological Measurements**

3  
4 **Rodrigo Shigueiro Siroma**

5 Department of Materials and Structures  
6 Université Gustave Eiffel, Bouguenais, Pays de la Loire, France, 44344  
7 rodrigo-shigueiro.siroma@univ-eiffel.fr

8  
9 **Mai Lan Nguyen**

10 Department of Materials and Structures  
11 Université Gustave Eiffel, Bouguenais, Pays de la Loire, France, 44344  
12 mai-lan.nguyen@univ-eiffel.fr

13  
14 **Pierre Hornych**

15 Department of Materials and Structures  
16 Université Gustave Eiffel, Bouguenais, Pays de la Loire, France, 44344  
17 pierre.hornych@univ-eiffel.fr

18  
19 **Tristan Lorino**

20 Department of Materials and Structures  
21 Université Gustave Eiffel, Bouguenais, Pays de la Loire, France, 44344  
22 tristan.lorino@univ-eiffel.fr

23  
24 **Yvong Hung**

25 Material Design Research Engineer  
26 TotalEnergies  
27 Solaize, Auvergne-Rhône-Alpes, France, 69360  
28 yvong.hung@totalenergies.com

29  
30 **Aurélia Nicolai**

31 R&D Project Manager  
32 Spie Batignolles Malet  
33 Portet-sur-Garonne, Midi-Pyrénées, France, 31120  
34 aurelia.nicolai@spiebatignolles.fr

35  
36 **Layella Ziyani**

37 Constructibility Research Institute  
38 École Spéciale des Travaux Publics, du Bâtiment et de l'Industrie  
39 Cachan, Île-de-France, France, 94234  
40 lziyani@estp-paris.eu

41  
42 **Emmanuel Chailleux**

43 Department of Materials and Structures  
44 Université Gustave Eiffel, Bouguenais, Pays de la Loire, France, 44344  
45 emmanuel.chailleux@univ-eiffel.fr

46  
47 Word Count: 6,956 words + 2 table (250 words per table) = 7,456 words

48  
49 *Submitted [August 1, 2021]*

1 **ABSTRACT**

2 The phase angle ( $\varphi$ ) has long been recognized as a powerful tool to detect variations in asphalt binders'  
3 chemical and microstructural properties. A recent study applied unsupervised multivariate approaches to  
4 uncover hidden pattern structures in data sets and settled the most relevant reduced frequency to  
5 investigate the evolution of the phase angle master curve with aging. Considering this recent study's  
6 findings, this paper revisits the  $\delta$ -method—i.e., an approach that estimates the Apparent Molecular  
7 Weight Distribution (AMWD) of a given asphalt binder based on its rheological behavior—and proposes  
8 a simple indicator that quantifies the incidence of asphaltene molecular agglomeration named Molecular  
9 Agglomeration Index (MAI). Laboratory- and field-aged binders were tested and a limiting value for MAI  
10 indicating an increased binder cracking susceptibility is established in agreement with other failure  
11 criteria found in the literature.

12 **Keywords:** Asphalt Binder Aging, Rheology,  $\delta$ -method, Failure criteria, Asphaltene agglomeration

1 **INTRODUCTION**

2 The positive social and economic impacts generated by roads are well-known despite the high  
3 investments required for their construction and maintenances. These infrastructures, however, only  
4 provide these benefits as long as their display enhanced serviceability in terms of comfort, safety, and  
5 reliability to the users. Therefore, to preserve these gains for longer, preventive maintenance must be done  
6 regularly and proactively (1); otherwise, roads can rapidly fall into disrepair. Despite the overall  
7 awareness that pavement preservation minimizes the entire lifecycle cost of a road, budgets of agencies,  
8 governments, and companies for this purpose have been restricted over the years (2). In this context,  
9 having reliable indicators that allow establishing either the optimal time or state from which asphalt  
10 materials display a critical point for intervention is of paramount importance to achieve the highest  
11 benefit-cost ratio, thus attenuating the limitations imposed by dwindling budgets.

12 Because of its desirable engineering characteristics, asphalt binder has long been the main  
13 binding agent employed in road construction (3). However, it is highly susceptible to oxidative aging  
14 when in contact with atmospheric oxygen due to its organic nature (3,4). Asphalt binder aging has long  
15 been considered as one of the key factors behind the major distresses of asphalt pavements and its impact  
16 on roads depends on various factors (5). In this case, the irreversible changes triggered by the aging  
17 phenomenon cause the asphalt binder to stiffen and embrittle, thus impairing the durability of pavements  
18 as the asphalt mixes therein become more prone to cracking.

19 Investigating chemical and microstructural changes in asphalt binders can provide valuable  
20 insights into how their mechanical behavior evolves. The increase in the concentration of polar functional  
21 groups with aging (6,7) favors intermolecular agglomeration (micelles) (4,8). This causes a reduction of  
22 mobility between molecules that grows the asphalt binder viscosity, which decreases the asphalt binders'  
23 ability to disperse mechanical and thermal stresses and thus increasing the cracking susceptibility of  
24 asphalt materials. The investigation of the microstructure of asphalt binders is usually performed via Gel  
25 Permeation Chromatography (GPC) that separates molecules by size. Laboratory- (6,9) and field-aging  
26 (10,11) yield a remarkable growth in the large molecular size. GPC, however, has some shortcomings  
27 (12–14). Moreover, breaking weak bonds between molecules during the elution may not only generate a  
28 curve that may not reflect the actual molecular weight distribution (MWD) of the original asphalt that is  
29 undiluted but also destroy potential clues that could provide valuable insights regarding the structural  
30 changes that take place in asphalt binder with aging.

31 The  $\delta$ -method (15,16) is an alternative to overcome the GPC limitations by estimating the MWD  
32 of a given asphalt binder based on its phase angle master curve. Rheology has proven to be very effective  
33 to assess the durability of asphalt binders since several specifications thereof are based on rheological  
34 indexes. Due to its high sensitivity, the phase angle has been widely recognized as a powerful indicator to  
35 detect variations in asphalt binders' chemical and structural properties (17,18). That said, (19) applied two  
36 unsupervised multivariate methods, which are used to uncover hidden pattern structures in data sets, to  
37 the phase angle master curves of aged asphalt binders. In this analysis, the asphalt binders were ordered  
38 correctly according to their aging level and grouped into two clusters that correspond satisfactorily with  
39 the Glover-Rowe (G-R) classification. Furthermore, one of the (19)'s findings is the determination of the  
40 most relevant reduced frequency to investigate the evolution of the phase angle master curves of  
41 unmodified asphalt binders with aging.

42 As the phase angle master curve is the core of both studies described, this work aims to revisit the  
43  $\delta$ -method with the findings presented in (19). A new index to quantify the incidence of molecular  
44 agglomeration through rheology is then proposed and applied to several laboratory- and field-aged asphalt  
45 binders. Lastly, a threshold value for this new index indicating an increased binder cracking susceptibility  
46 is established in agreement with some failure criteria found in the literature. It is noteworthy that since  
47 this work was conducted under the French national project "Modeling of Aging and Damage for  
48 Pavement Lifetime Assessment (MoveDVDC)", whose objective is to enhance the accuracy of current  
49 approaches for calculating the pavement remaining lifetime, all field-aged binders investigated were  
50 extracted and recovered exclusively from the asphalt base courses (ABCs) of thick pavement sites.

51

1 **MATERIALS**

2 An unmodified 35/50 pen grade asphalt binder (binder A) widely employed in road construction  
3 in France was subjected to different laboratory aging trials. On an asphalt scale, standard binder aging  
4 tests, i.e., Rolling Thin-Film Oven Test (RTFOT) and Pressure Aging Vessel (PAV), were used to  
5 simulate the short- and long-term aging, respectively. PAV was performed on the RTFOT-aged asphalt  
6 for 20 and 40 hours, named hereafter 1PAV and 2PAV, respectively.

7 On a loose asphalt mix scale, the aging protocol proposed by (20) was chosen. For this study, two  
8 sets of ‘*Grave Bitume* (GB3)’ asphalt mixes, commonly used in pavement base courses in France, were  
9 manufactured at 160°C in the laboratory using the same aforementioned fresh unmodified asphalt (Fresh).  
10 Limestone (Asphalt AL) and diorite (Asphalt AD) aggregates were utilized individually in each set of  
11 asphalt mixes to analyze the effect of different aggregates on the rheological indices used in this work.  
12 Soon thereafter (approximately 30 minutes later), the asphalt is extracted and recovered (After Mixing).  
13 Next, each of the loose asphalt mixes is laid and leveled in several pans to ensure a constant thickness of  
14 5–6 cm for short-term aging. These pans are then placed in a ventilated oven at 135°C for 4 hours, where  
15 the material is stirred for one minute every hour, thereby resulting in more homogenized aging. Once this  
16 step is done, the asphalt is extracted and recovered (4 hours at 135°C). The long-term aging consists of  
17 conditioning the short-term aged loose asphalt mix in a ventilated oven at 85°C, following the same  
18 procedures described to obtain a good homogenization, for 2, 5, 7, 9, and 20 days, where at each aging  
19 level, the asphalt binders (2 days), (5 days), (7 days), (9 days), and (20 days), respectively, are extracted  
20 and recovered from the loose asphalt mix to be characterized.

21 Full-depth field samples were cored vertically in 2020 from two thick pavement sites whose  
22 ABCs are GB3 mixes formulated with unmodified 35/50 pen binders: A35 highway and Test Track B of  
23 the Université Gustave Eiffel’s Fatigue Carrousel. A35 highway was built in 2002 and the section from  
24 which the field cores were taken is near Strasbourg (northeastern France), i.e., in a continental climate.  
25 A35 highway structure consists of a 6 cm asphalt wearing course, a 12 cm ABC with 40% of reclaimed  
26 asphalt pavement (RAP), and another 12 cm ABC without RAP. As for Fatigue Carrousel’s Test Track B  
27 built in 1998 and located under an oceanic climate near Nantes (Western France), the pavement structure  
28 consists of an 8 cm asphalt wearing course, a 6 cm ABC, and 2 identical ABCs of 15 cm each. For this  
29 specific site, the availability of rheological data of the fresh asphalt binder used during the construction of  
30 the base courses, as well as the RTFOT-aged binder, allows the assessment of the evolution of the  
31 rheological parameters over the past 22 years. In both sites, field cores were extracted from both  
32 trafficked (below the wheel path) and untrafficked (outside the wheel path) zones to assess the possible  
33 influence of traffic loading on the properties of the field-aged binders. Binders were extracted and  
34 recovered from the two ABCs of A35 highway (base courses 1 and 2) and two deeper ABCs that compose  
35 Test Track B (base courses 2 and 3), as presented in (**Figure 1**), where special caution was taken to  
36 prevent tack and prime coats materials from contaminating the extracted binders by cutting them off  
37 previously. Despite the awareness of the greater severity of aging near the pavement surface, the  
38 MoveDVDC project focuses rather on the evolution of the asphalt mix in ABC as, unlike the upper layers  
39 that can be replaced, ABC lasts throughout the whole pavement lifespan.

40

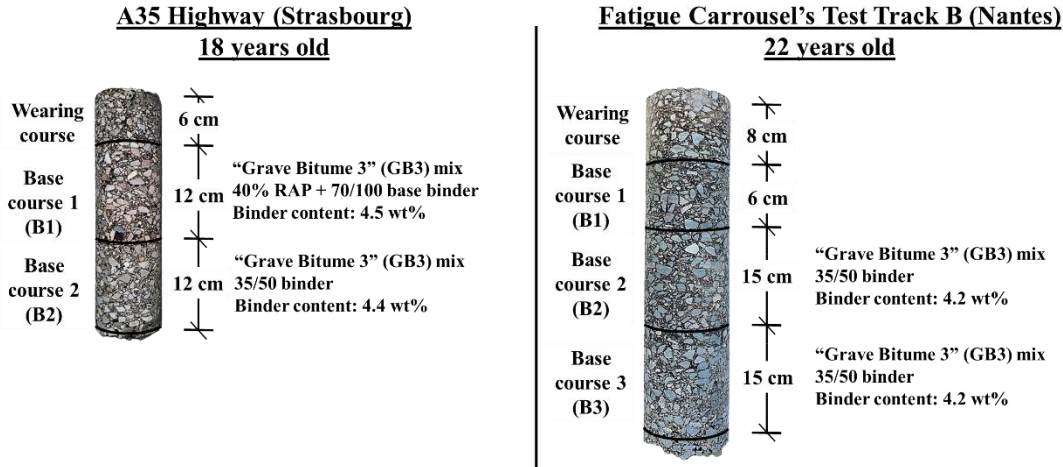


Figure 1 Field cores from A35 Highway (Strasbourg) and Test Track B (Nantes)

In addition, 19 supplementary rheological datasets were taken from (21) and (22) to enrich the analysis proposed in this paper. All asphalt binders used are shown in Table 1.

TABLE 1 Summary of all binders used in this work

Agging Type	Sample	Agging level	Supplementary information
Laboratory-aged binder (Rheometer: Metravib®)	A Fr	Fresh	Unmodified 35/50 pen grade
	A RT	RTFOT	
	A 1P	1PAV (20 h PAV)	
	A 2P	2PAV (40 h PAV)	
Extracted and recovered from laboratory-aged loose mixes (GB3)  (Rheometer: Metravib®)	AD Fr	Fresh	GB3 mix formulated with unmodified 35/50 pen binder and diorite aggregates
	AD Mix	After mixing	
	AD 4h	4 hours at 135°C	
	AD 2d	2 days at 85°C	
	AD 5d	5 days at 85°C	
	AD 7d	7 days at 85°C	
	AD 9d	9 days at 85°C	
	AD 20d	20 days at 85°C	
	AL Fr	Fresh	GB3 mix formulated with unmodified 35/50 pen binder and limestone aggregates
	AL Mix	After mixing	
AL 4h	4 hours at 135°C		
AL 2d	2 days at 85°C		
Extracted and recovered from the base courses (GB3) of field cores  (Rheometer: Metravib®)	S B1U	18 years (field aging)	Strasbourg, Base course 1, Untrafficked
	S B1T	18 years (field aging)	Strasbourg, Base course 1, Trafficked
	S B2U	18 years (field aging)	Strasbourg, Base course 2, Untrafficked
	S B2T	18 years (field aging)	Strasbourg, Base course 2, Trafficked
	N Fr	Fresh	Unmodified 35/50 pen grade
	N RT	RTFOT	
	N B2U	22 years (field aging)	

	N B2T	22 years (field aging)	Nantes, Base course 2, Trafficked
	N B3U	22 years (field aging)	Nantes, Base course 3, Untrafficked
	N B3UT	22 years (field aging)	Nantes, Base course 3, Trafficked
Laboratory-aged binders from (22)  (Rheometer: Metravib®)	K1 Fr	Fresh	Unmodified 10/20 pen grade
	K1 RT	RTFOT	
	K1 1P	1PAV (20 h PAV)	
	K2 Fr	Fresh	Unmodified 20/30 pen grade
	K2 RT	RTFOT	
	K2 1P	1PAV (20 h PAV)	
	K3 Fr	Fresh	Unmodified 35/50 pen grade
	K3 RT	RTFOT	
	K3 1P	1PAV (20 h PAV)	
	K4 Fr	Fresh	Unmodified 50/70 pen grade
	K4 RT	RTFOT	
	K4 1P	1PAV (20 h PAV)	
Extracted and recovered from laboratory-aged loose mixes (GB3) (21) Rheometer: Dynamic Shear Rheometer (DSR)	T Fr	Fresh	GB3 mix formulated with unmodified 35/50 pen binder and gneiss aggregates
	T Mix	After mixing	
	T 4h	4 hours at 135°C	
	T 2d	2 days at 85°C	
	T 5d	5 days at 85°C	
	T 7d	7 days at 85°C	
	T 9d	9 days at 85°C	

1

## 2 METHODS

### 3 Frequency sweep test

4 Frequency sweep tests at multiple temperatures were conducted in a Metravib® rheometer.  
 5 Asphalt binder's complex modulus and phase angle ( $\varphi$ ) were measured at 1–80 Hz at several  
 6 temperatures, ranging from -15 to 60°C, in displacement (strain) control mode. Unlike the DSR,  
 7 rheological measurements in a Metravib® rheometer are obtained in tension-compression mode ( $E^*$ ) at  
 8 low temperatures, from -15 to 20°C, and annular shear mode ( $G^*$ ) at high temperatures, from 20 to 60°C.  
 9 The conversion from  $|G^*|$  to  $|E^*|$  or vice versa is made considering a Poisson's ratio of 0.5. A minimum of  
 10 two replicates was performed for each sample as long as the coefficients of variation (CV) of  $E^*$  and  $\varphi$   
 11 are lower than 15% and 5%, respectively.

12

### 13 Rheological data treatment

#### 14 Master curve construction

15 When submitted to a small number of cycles whose strain or stress magnitude is kept small  
 16 enough, asphalt binder can be regarded as a thermo-rheologically simple linear viscoelastic (LVE)  
 17 material (23,24). In this domain, the limitations of laboratory testing conditions can be overcome with  
 18 unique master curves of complex modulus ( $|G^*|$  to  $|E^*|$ ) and phase angle ( $\varphi$ ) at a given reference  
 19 temperature ( $T_{ref}$ ) that allows extrapolation of experimental data to more realistic situations.

20 Among the several methods found in the literature to compute the shift factors ( $a_T$ ) for each  
 21 isotherm, the mathematical-based master curve construction method (25) was employed. Based on the  
 22 Kramer-Kronig relation between the real and imaginary components of complex functions (26), the shift  
 23 factors for each isotherm can be computed by **Equation 1**:

24

$$25 \quad \log(a_{T(T_i, T_{ref})}) = \sum_{j=1}^{j=ref} \frac{\log(|E^*(T_j, \omega)|) - \log(|E^*(T_{j+1}, \omega)|)}{\varphi_{avg}[(T_j, T_{j+1}), \omega]} \quad (1)$$

1  
2 where

3  $a_{T(T_i, T_{ref})}$  = shift factor of an isotherm at  $T_i$  in relation to the  $T_{ref}$ ;  
4  $|E^*(T_j, \omega)|$  = complex modulus norm at a given temperature  $T_j$  and frequency  $\omega$ ; and  
5  $\varphi_{avg}$  = mean value of the phase angles at  $T_j$  and  $T_{j+1}$  both at a given frequency  $\omega$ .  
6

7 In this study, the master curves of all binders were built at a reference temperature of 0°C.  
8

9 *2 Spring, 2 Parabolic elements, and 1 Dashpot (2S2PID) rheological model*

10 The analogical LVE 2S2PID model (27) was used to fit rheological raw data. The complex  
11 modulus is given by Equation 2:  
12

$$13 \quad E^*(i\omega\tau) = E_0 + \frac{E_\infty - E_0}{1 + \delta(i\omega\tau)^{-k} + (i\omega\tau)^{-h} + (i\omega\beta\tau)^{-1}} \quad (2)$$

14 where,

15  $E^*(i\omega\tau)$  = complex modulus;  
16  $i$  = imaginary unit;  
17  $\omega$  = solicitation pulsation;  
18  $E_0$  = static modulus ( $E_0 = 0$  for binders);  
19  $E_\infty$  = glassy modulus;  
20  $\delta$  = dimensionless calibration constant;  
21  $k$  = ratio  $E_{imaginary}/E_{real}$  when  $\omega$  tends to 0;  
22  $h$  = ratio  $E_{imaginary}/E_{real}$  when  $\omega$  tends to  $\infty$ ;  
23  $\beta$  = Newtonian viscosity; and  
24  $\tau$  = characteristic time.  
25  
26

27 **Findings of works highlighting the importance of the phase angle master curves**

28  *$\delta$ -method*

29 Before actually starting this subsection, to avoid confusion, this will be the only subsection where  
30 the phase angle will be referenced by “ $\delta$ ” due to the name of the method. After this subsection, the phase  
31 angle will again be referenced by the Greek letter “ $\varphi$ ” to avoid confusion with the dimensionless  
32 parameter ( $\delta$ ) of the 2S2PID model (Equation 2).

33 According to (16), a given material undergoes several relaxation processes when subjected to  
34 dynamic loadings. Against this background, this material can be regarded as a mixture of monodisperse  
35 molecular weight species. In this case, each of them displays a unique relaxation frequency below which  
36 this species relaxes and does not contribute to the mechanical response of the material, thus causing the  
37 modulus to reduce and, consequently, the phase angle to increase. In this scenario, the already relaxed  
38 species act as a diluent for the non-relaxed components. On the other sense, the higher the loading  
39 frequency, the smaller the molecules that contribute to the material’s mechanical resistance and thereby  
40 increasing the elastic contribution of the complex modulus. Furthermore, the smaller the particles the  
41 shorter is the reaction time to external loads, thus reducing the phase angle.

42 Grounded in this hypothesis, (16) stated that the phase angle seems to be the most sensitive  
43 rheological parameter to determine the AMWD. Calibration was then done between the crossover  
44 frequency ( $\omega_c$ ) at  $T = 0^\circ\text{C}$  and the molecular weight (MW) measured by Vapor Pressure Osmometry of  
45 several regular binders from the Strategic Highway Research Program (SHRP) library and also Alberta  
46 crude oils, where the following equation was proposed:  
47

1  $\log(MW) = 2.880 - 0.06768 \log(\omega_c)$  (3)

2 Following up (16), (15) employed Equation 3 to plot the phase angle master curve as a function  
 3 of molecular mass (MW). Considering the hypothesis presented, the Cumulative Molecular Weight  
 4 Distribution (CMWD) is proportional to the phase angle master curve ( $\delta$ ) and is given by Equation 4:  
 5

6  $CMWD = \frac{1}{90^\circ} \delta(MW)$  (4)

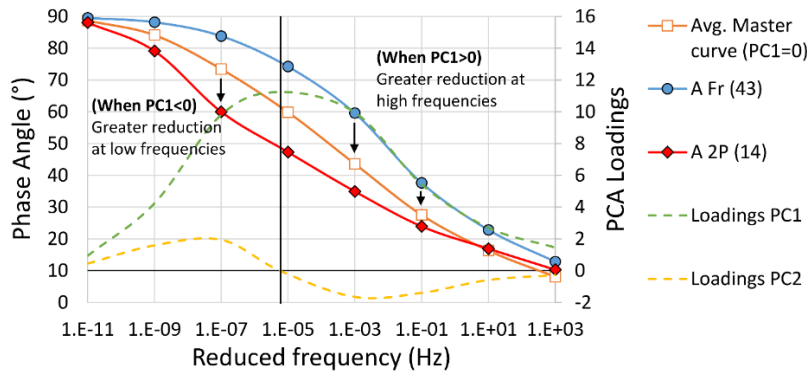
7  
 8 The derivative of the CMWD will finally result in the AMWD equation:  
 9

10  $AMWD = \frac{d(CMWD)}{d(\log(MW))} \cong \frac{\Delta(CMWD)}{\Delta(\log(MW))}$  (5)

11 where a step size of 1/3.000 was suggested by (21) to facilitate the convergence of the numerical  
 12 derivative. An alternative to calculating the AMWD is described in (22), where an analytical equation  
 13 using the rheological parameters of the 2S2P1D model is proposed.  
 14

15 *Application of multivariate statistical analyses*

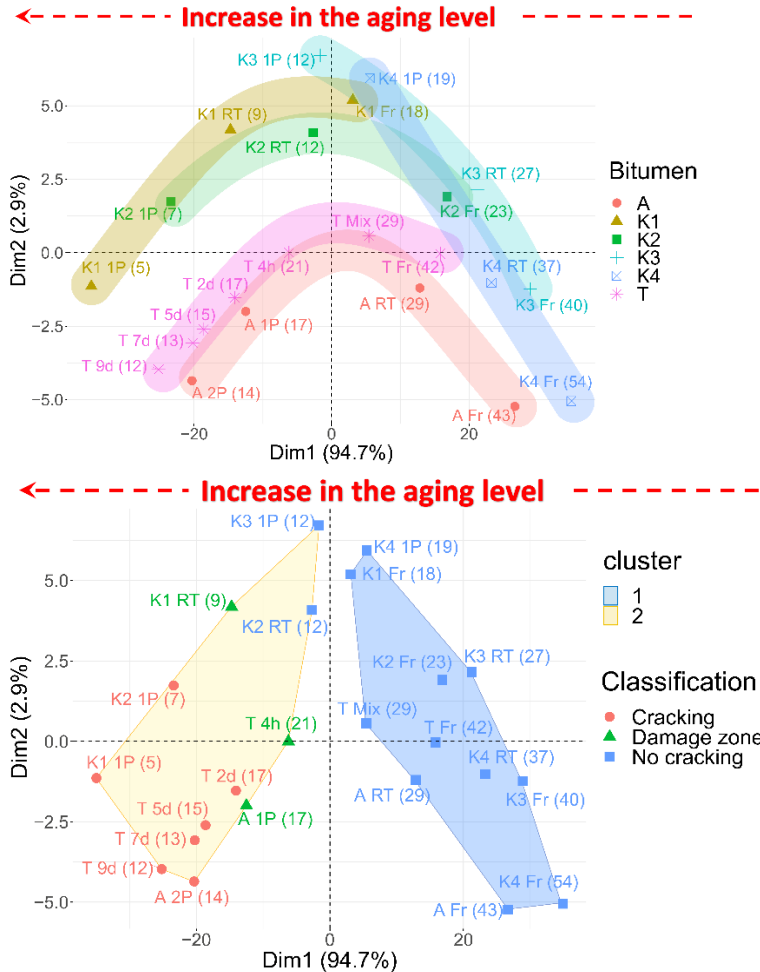
16 Widely employed in several science fields to detect hidden phenomena implied in data sets,  
 17 Principal Component Analysis (PCA) reduces the dimensionality of a data set with minimal loss of  
 18 information and thereby increase interpretability. For this, the original data set is replaced by new  
 19 variables uncorrelated (orthogonal) to each other called principal components (PCs) that are linear  
 20 combinations of the original variables. The first PC (PC1) corresponds to the direction that explains the  
 21 most variation of the original data set within the multidimensional space. Orthogonally to PC1, PC2  
 22 accounts for the largest variation that has not been considered by PC1. Subsequent PCs are determined  
 23 likewise. Usually used as a complement of PCA, Hierarchical Cluster Analysis (HCA) groups individuals  
 24 according to their similarities (distances) between them. In this case, (19) applied both methods (PCA and  
 25 HCA) using 8-well-distributed points represented by the markers along the phase angle master curves  
 26 (**Figure 2**) to classify and also cluster binder based on their aging levels as shown in (**Figure 3**).



27  
 28 **Figure 2** Markers representing the 8-well-distributed points along the phase angle master curves  
 29 used for the PCA analysis and the PC1 and PC2 loadings (dashed lines) indicating the importance  
 30 of each reduced frequency on each PC (19)  
 31

32 The PCA score plot (**Figure 3 top**) presents that the PC1 (horizontal axis) describes 94.7% of the  
 33 total variation whereas PC2 (vertical axis) accounts for 2.9%. It is observed that the binders were sorted  
 34 along PC1, from right (fresher binders) to left (more aged binders), where a marked inflection point can  
 35 be seen when the binders cross the vertical axis. All the studied binders were grouped into two clusters

1 through HCA, one on each side of the inflection point. **(Figure 3 bottom)** shows that the output of the  
 2 PCA and then HCA analyses correspond satisfactorily with the G-R classification. One of the key  
 3 findings of this work is the determination of the value of  $5.7 \times 10^{-6}$  Hz as the most important reduced  
 4 frequency for PC1 as shown by the PC1 loadings in **(Figure 2)** and also the balance below and above this  
 5 value results in the inflection point observed.  
 6



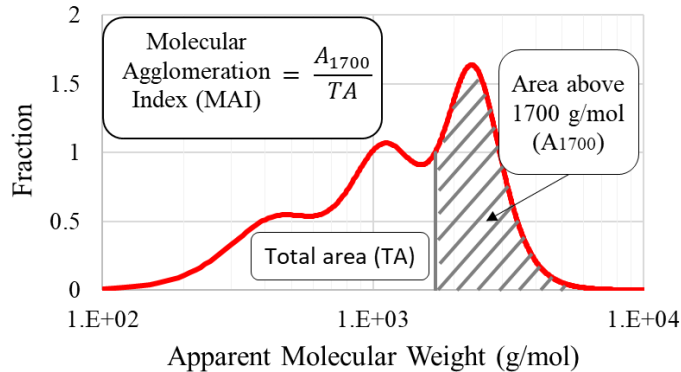
10 **Figure 3** PCA score plot (top) and the two HCA clusters where the individuals are color-coded  
 11 according to their G-R classification (19)  
 12

13 **Molecular Agglomeration Index (MAI)**

14 A relationship between the finding of the application of the multivariate statistical analyses (PCA  
 15 and HCA) (19) and the  $\delta$ -method (15) can be established since both are grounded in the phase angle  
 16 master curve at a reference temperature of  $0^{\circ}\text{C}$ . The PCA analysis highlighted the value of  $5.7 \times 10^{-6}$  Hz  
 17 and according to Equation (3), proposed by (16), this corresponds to approximately 1,700 g/mol. The fact  
 18 that the molecular weight of asphaltene is 500–1,000 g/mol (28), this value may correspond with the  
 19 incidence of asphaltene agglomeration, which may also be a key value indicating the sol-gel transition.

20 Aiming to quantify the incidence of the asphaltene molecular agglomeration, this study proposes  
 21 a straightforward method that consists of dividing the area below the AMWD above 1,700 g/mol by the  
 22 total area (from  $10^2$  to  $10^4$  g/mol). MAI is illustrated in **(Figure 4)** and varies from 0 to 1, where the closer  
 23 to 1, the greater the incidence of agglomerated molecules in the studied binder. As stated by (8), the  
 24 delicate balance, or the lack of it, between associated or agglomerated components and dispersed or

1 solubilized components impacts strongly on the performance of asphalt binders. It is worth mentioning  
 2 that MAI is a shape parameter since it takes into account the entire phase angle master curve.  
 3



4  
 5  
 6 **Figure 4 Molecular Agglomeration Index (MAI)**

7  
 8 **Failure criteria based on frequency sweep test**

9 The high susceptibility to thermal variation and loading duration displayed by asphalt materials  
 10 has strongly encouraged the routine use of rheological parameters for binder specification. Based  
 11 generally on properties of binder extracted and recovered from roads whose cracking incidence was  
 12 known, some criteria have been proposed as possible indicators of asphalt binder durability.  
 13

14 *Glover-Rowe (G-R) parameter*

15 Considered as an intermediate temperature criterion, the G-R parameter (29) has widely been  
 16 employed to assess the non-load-associate cracking propensity of asphalt materials and is expressed as  
 17 follows:

18 
$$G-R = \frac{|G^*|(\cos\varphi)^2}{\sin\varphi} \quad (6)$$

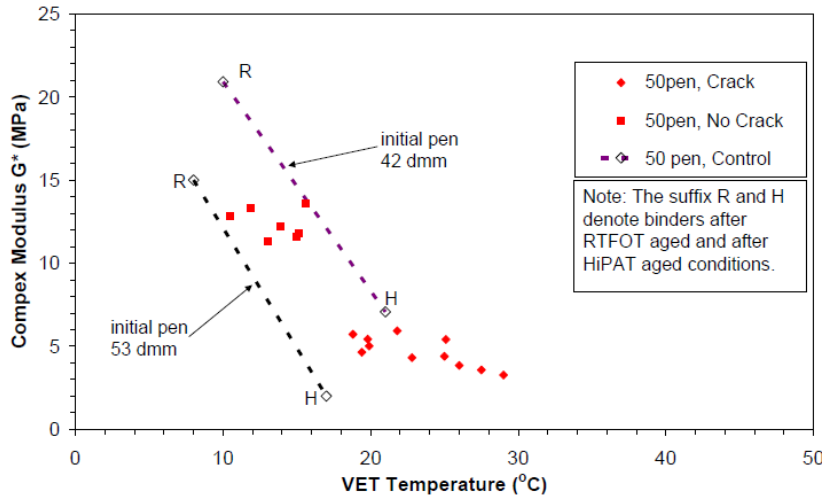
19 where  $|G^*|$  and  $\varphi$  are the complex modulus norm and phase angle, respectively, measured at 15°C and  
 20 0.005 rad/s. According to this parameter, the damage onset and significant cracking susceptibility due to  
 21 non-load-related cracking are likely to arise when the value computed is higher than 180 and 600 kPa,  
 22 respectively.  
 23

24 *Limiting temperatures corresponding to the 27° and 45° phase angles*

25 Several surveys conducted in the 1990s on several 7-year-old French roads built with 35/50 pen  
 26 grade binders showed a good correlation of the surface cracking incidence and temperatures  
 27 corresponding to the phase angles of 27° and 45° at 7.8 Hz (30,31). Both criteria increase with aging and  
 28 the threshold values of  $T_{(\varphi=27^\circ)} = 12^\circ\text{C}$  and  $T_{(\varphi=45^\circ)} = 35^\circ\text{C}$ , both at 7.8 Hz, were set for unmodified 35/50  
 29 pen grade binders, which correspond to those measured in the field-binders extracted and recovered from  
 30 cracked zones after 7 years of service.

31 Inspired by the  $T_{(\varphi=45^\circ)}$  indicator proposed initially in France (30), the so-called Visco-Elastic  
 32 Transition Temperature ( $T_{\text{VET}}$ ) is an indicator based on binders from several aged roads across the United  
 33 Kingdom that corresponds to the  $T_{(\varphi=45^\circ)}$  at 0.4 Hz (32). In the  $G^*_{\text{VET}}$  versus  $T_{\text{VET}}$  plot, the binders used in  
 34 (32,33) fall within different zones that reflect satisfactorily the performance level observed in these sites,  
 35 as shown in (Figure 5). Both studies conclude that the  $G^*_{\text{VET}}$  versus  $T_{\text{VET}}$  graph seems to be a useful  
 36 preliminary screening tool for assessing the cracking susceptibility of binders. Moreover, (32) proposed  
 37 limiting values of  $T_{\text{VET}}$  for 15 and 50 pen grade binders corresponding to poor performing sites at 0.4 Hz,  
 38 which have yet to be validated:

- 1 • For 15 pen grade:  $T_{VET} > 35^{\circ}\text{C}$  and  $G^*_{VET} < 5 \text{ MPa}$ ; and
- 2 • For 50 pen grade:  $T_{VET} > 20^{\circ}\text{C}$  and  $G^*_{VET} < 10 \text{ MPa}$ .
- 3

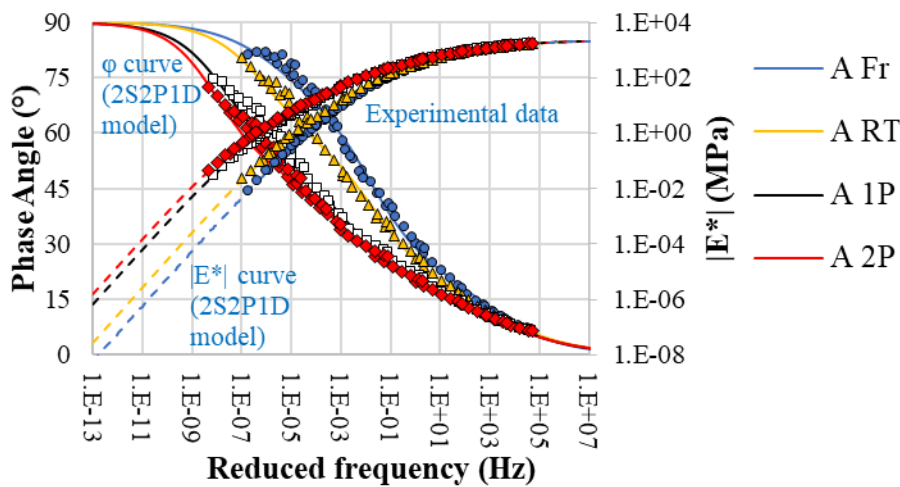


4  
5  
6 **Figure 5 Mapping 50 pen binders recovered from stone mastic asphalt mixes (cracked and non-**  
7 **cracked sites) and ‘control’ binders at 0.4 Hz (32)**

8 **RESULTS AND DISCUSSION**

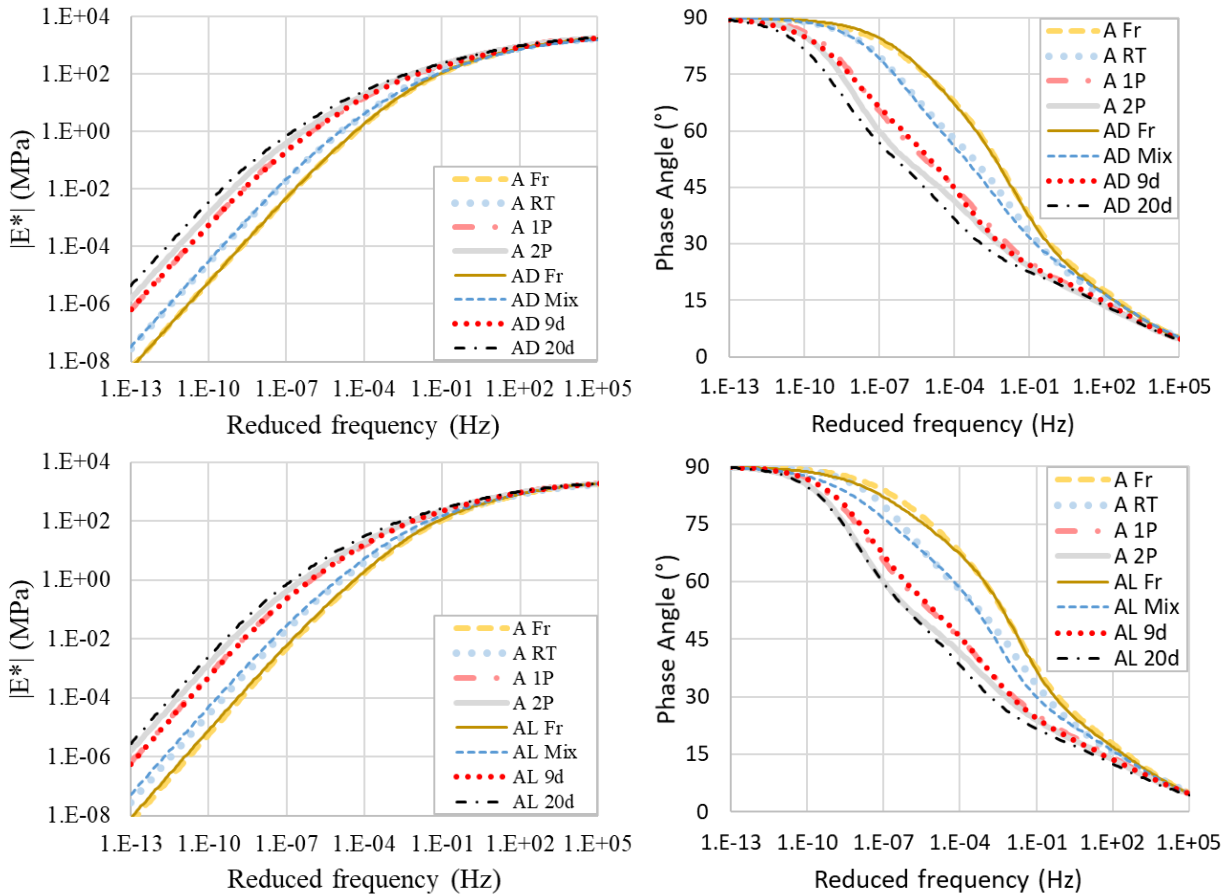
9 **Rheological measurements**

10 All asphalt binders had their experimental data satisfactorily fitted with the 2S2P1D rheological  
11 model as shown in (Figure 6), thus allowing the use of this model for the analyses proposed in this study.  
12 (Figure 6) shows the well-known trend in the evolution of asphalt rheology with aging: the increase in  
13 complex modulus (dashed lines) mainly in conditions under which the asphalt previously displayed a  
14 more viscous-like behavior, i.e., at high temperatures and/or low frequencies, results in an overall  
15 reduction of its phase angle (solid lines), indicating an increasingly elastic and less viscous material.



19  
20  
21 **Figure 6 Evolution of the complex modulus (dashed lines) and phase angle (solid lines) master**  
22 **curves of the laboratory-aged binder A (19)**

1 Since asphalt binders A, AD, and AL are from the same batch but aged differently, an attempt to  
 2 correlate their aging levels based on the similarities of their master curves is illustrated in **(Figure 7)**. The  
 3 complex modulus master curves of binders A Fr, A RT, and A 1P seem to be completely superimposed  
 4 on these corresponding to the fresh, after mixing, and after 9-day aging, respectively, of binders AD and  
 5 AL. The complex modulus master curve of binder A 2P is halfway between the curves corresponding to  
 6 9- and 20-day aging levels of both AD and AL.  
 7



8

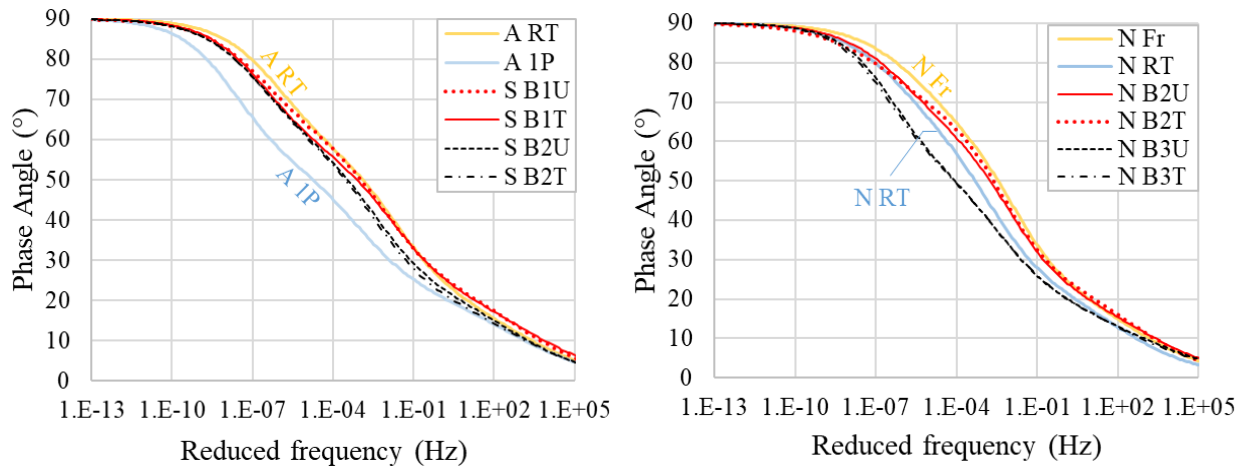
9

10

11 **Figure 7 Comparison between the complex modulus (left) and phase angle (right) master curves of**  
 12 **binders A and AD (top); and between binders A and AL (bottom)**  
 13

14 The phase angle master curve appears to be more sensitive in distinguishing binders as seen in  
 15 **(Figure 7)**. The phase angle master curve of the field-aged binders from the base courses of the pavement  
 16 sites Strasbourg (S) and Nantes (N) is presented in **(Figure 8)**. Given the lack of initial data of the binders  
 17 used during the construction of site S, the phase angle master curves of binders A RT and A 1P were  
 18 inserted as a reference level of aging. The binders from base courses 1 and 2 are found between the curves  
 19 corresponding to binders A RT and A 1P, where binders S B2U and S B2T are more aged than binders S  
 20 B1U and S B1T. It is also observed that there are practically no differences between the trafficked and  
 21 untrafficked zones. As for the binders from the Fatigue Carrousel's Test Track B in Nantes, binders N  
 22 B2U and N B2T seem to have barely evolved over the last 22 years, as their phase angle master curves  
 23 are still close to that of N Fr. Binders N B2U and N B2T seem to be less aged than N RT (RTFOT-aged  
 24 binder), which can be explained by the high aggressiveness of the RTFOT protocol usually discussed in  
 25 the literature (34). It is also observed that the binders N B3U and N B3T extracted from the deeper course  
 26 are harder than those extracted from the middle course (binders N B2U and N B2T).

1



2

3

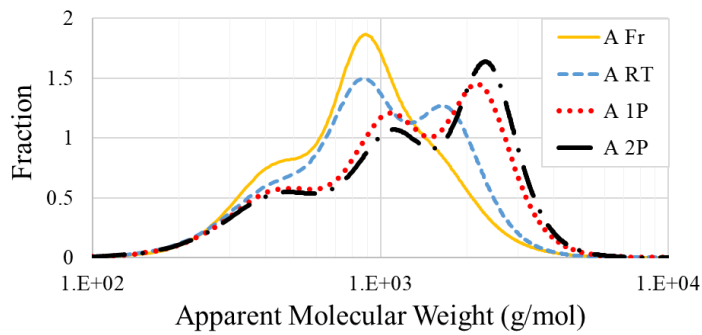
4 **Figure 8 Phase angle master curves of field-aged binders from A35 highway (Strasbourg) and Test**  
 5 **Track B (Nantes)**

6

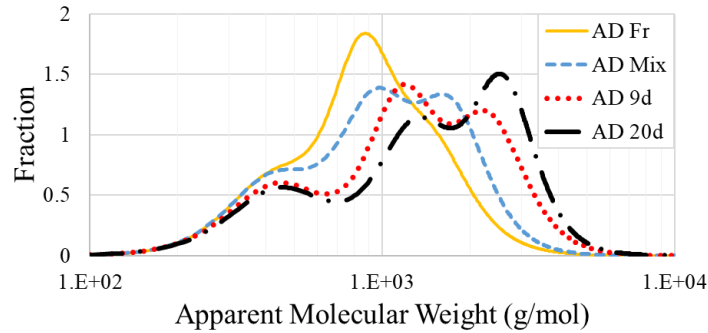
7 **Evolution of the AMWD with aging**

8 The AMWDs obtained from the rheological data of the binders at each aging level through the  $\delta$ -  
 9 method are portrayed in (Figure 9). Binders A Fr (top), AD Fr (middle), and AL Fr (bottom) display a  
 10 unimodal distribution-shaped AMWD centered at around 900 g/mol. With aging, the AMWDs initially  
 11 take on a bimodal and then a trimodal distribution-shaped where a marked shift toward higher molecular  
 12 weights and the creation of a new molecular population are observed, such as the peak around 2.000  
 13 g/mol that may represent asphaltene molecules agglomeration (15,21,22).

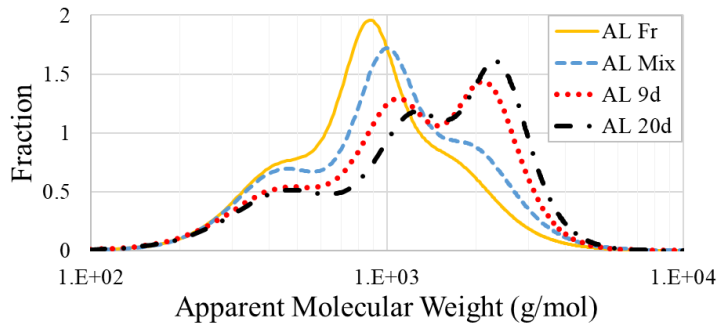
14



15

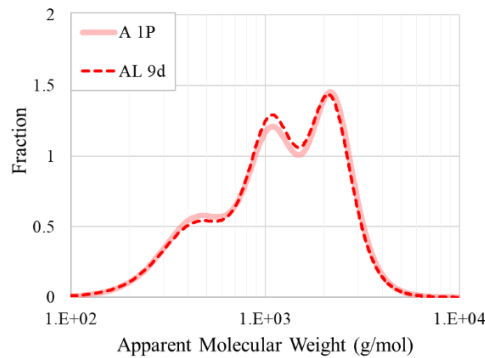
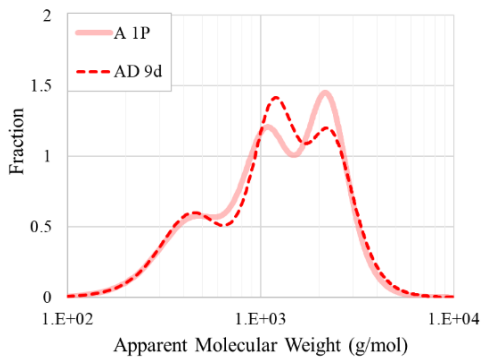
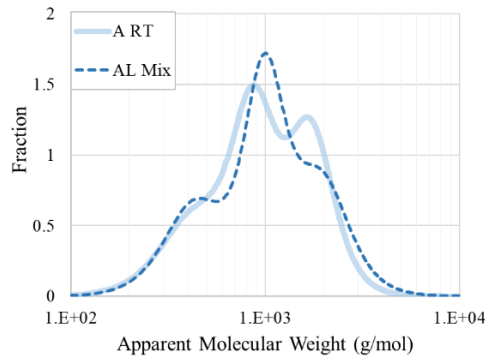
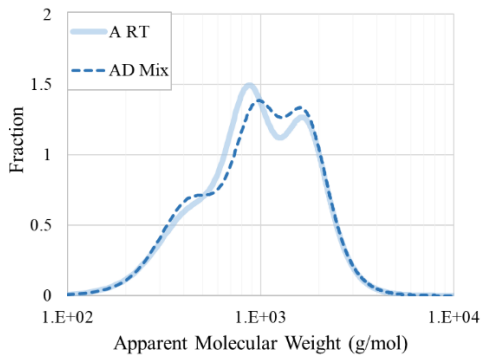
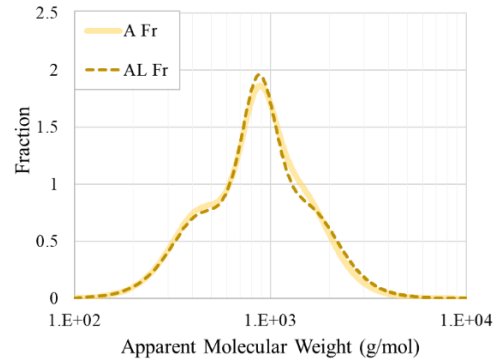
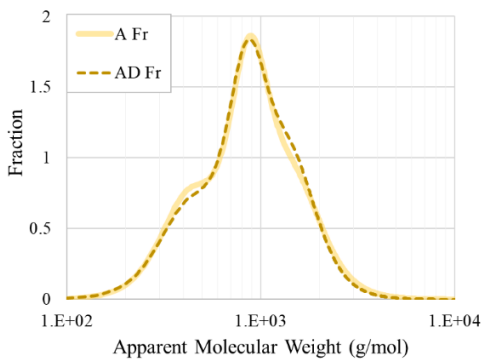


16



1 **Figure 9** AMWDs determined through  
 2 **the  $\delta$ -method for binders A (top), AD (middle), and AL (bottom)**  
 3

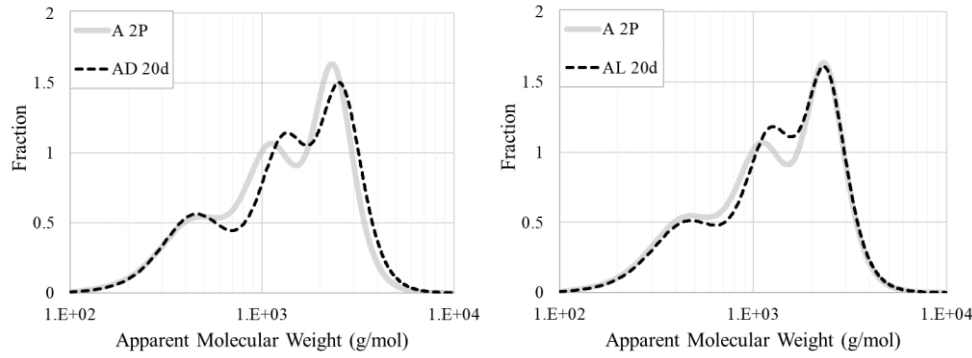
4 **(Figure 10)** presents the AMWDs of the aging states whose phase angle master curves  
 5 correspond well to each other in Figure 7. The  $\delta$ -method can also be employed to highlight possible  
 6 rheological differences that can sometimes go unnoticed when using traditional graphical representations.  
 7 Given its high sensitivity, the method could be used for binder fingerprinting as long as a good fit of the  
 8 rheological model to the experimental data is ensured.



9

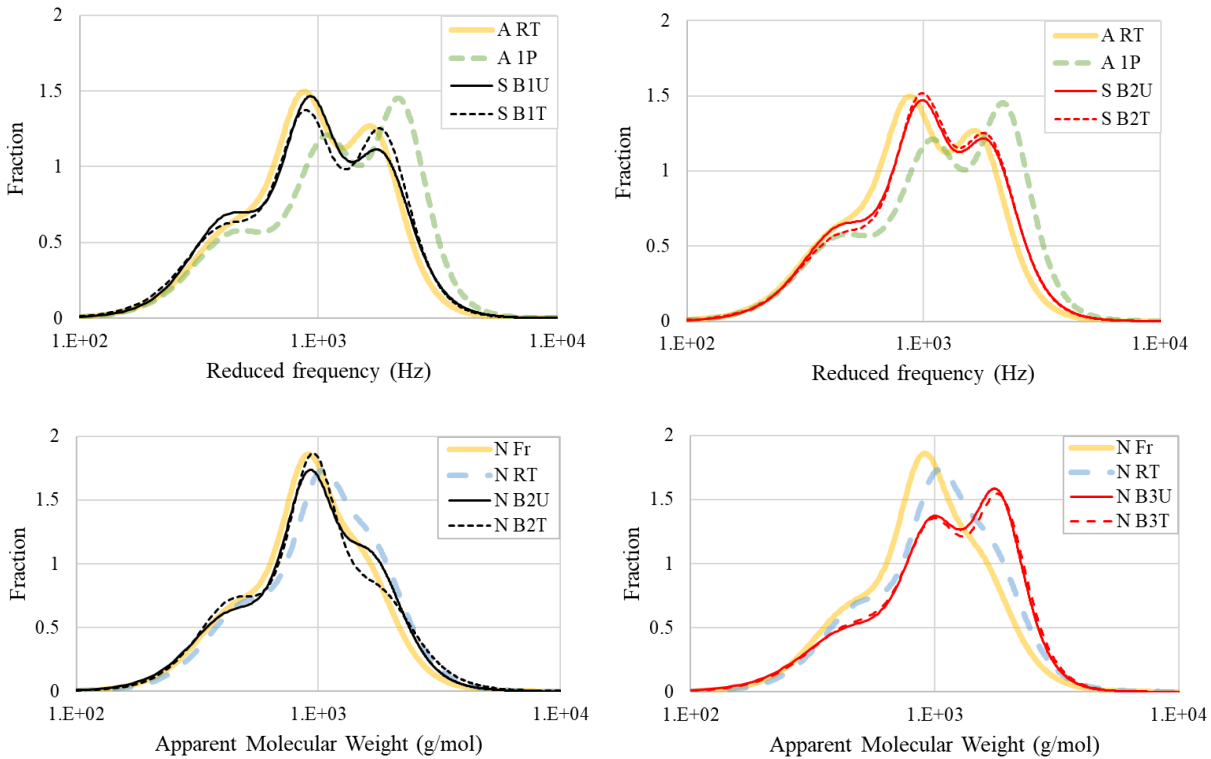
10

11



1  
2 **Figure 10 Comparison of the AMWDs of binders whose phase angle master curves overlap**  
3 **reasonably well with each other**

4  
5 The AMWDs of the field-aged binders from the pavements sites Strasbourg (S) and Nantes (N)  
6 are shown in (Figure 11). For both sites, the trend is similar to that seen in (Figure 8); however, due to  
7 the greater sensitivity of the  $\delta$ -method, it is possible to observe small differences between the curves. In  
8 this case, the AMWDs corresponding to the binders extracted from trafficked zones, mainly in the upper  
9 ABC, seems to be slightly shifted toward higher molecules (i.e., more aged binder).



12  
13  
14 **Figure 11 AMWD of field-aged binders from the pavement sites Strasbourg (S) (top) and Nantes**  
15 **(N) (bottom)**

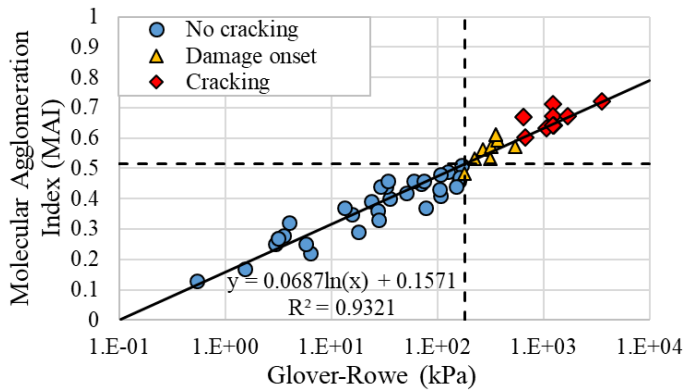
16  
17 Despite being a powerful tool that provides valuable insights for a better understanding of the  
18 changes caused by asphalt binder aging, the analysis of only AMWDs is insufficient. Some attempts to  
19 quantify the evolution of the AMWD with possible molecular populations are presented in (15,21,22), In

1 (15), 3 molecular populations were states as integrating the AMWD whereas in (21,22) 4 molecular  
 2 populations were fixed and deconvoluted into 4 gaussian functions. These two last-mentioned studies  
 3 stated that the main change in binder AMWD triggered by aging occurs at 2.000 g/mol, which is in line  
 4 with the Molecular Agglomeration Index (MAI) proposed in this work.

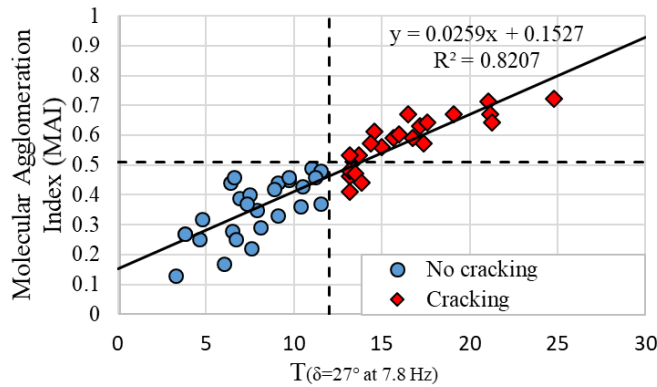
5

6 **Failure criteria based on frequency sweep test**

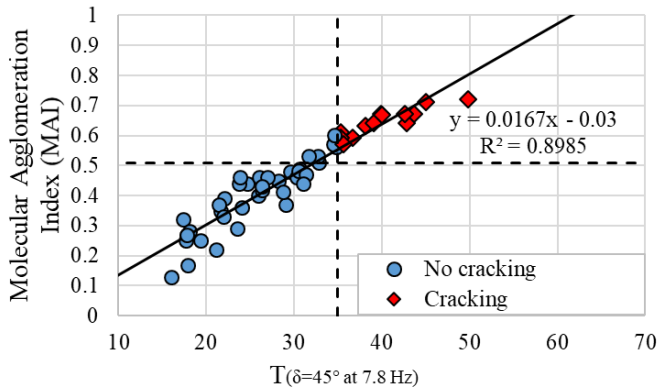
7 (Figure 12) shows that the evolution of MAI correlates satisfactorily with that of the G-R as well  
 8 as  $T_{(\varphi=27^\circ)}$  and  $T_{(\varphi=45^\circ)}$  at 7.8 Hz. In this case, a threshold value that will indicate the state from which a  
 9 given asphalt binder displays an increased cracking susceptibility will be set based on these 3 criteria. For  
 10 each criterion, the values obtained for MAI are slightly different, varying from 0.46 to 0.55. The limiting  
 11 value settled for MAI is then 0.51 (average value), corresponding approximately to G-R = 170.2 kPa,  
 12  $T_{(\varphi=27^\circ \text{ at } 7.8\text{Hz})} = 13.8^\circ\text{C}$ , and  $T_{(\varphi=45^\circ \text{ at } 7.8\text{Hz})} = 32.3^\circ\text{C}$ .



13



14



15

16 **Figure 12 Correlation of MAI with the G-R (top),  $T_{(\varphi=27^\circ)}$  at 7.8 Hz (middle), and  $T_{(\varphi=45^\circ)}$  at 7.8 Hz**  
 17 **(bottom)**

18

The analysis of the  $T_{VET}$  at 0.4 Hz showed that the classification of the studied binders is very similar to that of the  $T_{(\varphi=45^\circ)}$  at 7.8 Hz, where the only difference is the temperature under which this targeted phase angle of  $45^\circ$  is found. Since the  $T_{VET}$  at 0.4 Hz proposed by (32) has no limiting values for 35/50 pen grade binders, the same analysis for MAI described above was performed and a tentative failure criterion for the  $T_{VET}$  at 0.4 Hz for 35/50 pen grade asphalt binders is then proposed:  $T_{VET} > 22^\circ\text{C}$  and  $G^*_{VET} < 7 \text{ MPa}$ . It is interesting to note that these proposed values are between the failure values defined by (32) for 15 and 50 pen binders. (**Table 2**) summarizes all the failure criteria for the binders used in this work.

**TABLE 2 Summary of the results of all the failure criteria used in this work (values in italic indicate the damage onset according to the G-R parameter, while those in bold indicate an increased cracking susceptibility according to each criterion used)**

Aging Type	Sample	G-R (kPa)	$T_{(\varphi=27^\circ)}$ at 7.8 Hz ( $^\circ\text{C}$ )	$T_{(\varphi=45^\circ)}$ at 7.8 Hz ( $^\circ\text{C}$ )	$T_{VET}$ at 0.4 Hz ( $^\circ\text{C}$ )	$G^*_{VET}$ at 0.4 Hz (MPa)	MAI
Laboratory-aged binder	A Fr	3.17	3.8	17.8	8.2	17.98	0.27
	A RT	23.79	6.9	22.1	12.3	12.90	0.39
	A 1P	<i>357.82</i>	<b>14.6</b>	<b>35.4</b>	<b>24.5</b>	<b>5.20</b>	<b>0.61</b>
	A 2P	<b>647.05</b>	<b>16.5</b>	<b>40.0</b>	<b>28.9</b>	<b>3.32</b>	<b>0.67</b>
Laboratory-aged loose asphalt mix (GB3) with diorite aggregates	AD Fr	2.98	4.6	17.7	8.3	18.19	0.25
	AD Mix	35.28	7.5	25.9	15.6	8.05	0.40
	AD 4h	70.21	9.7	28.2	17.9	7.58	0.45
	AD 2d	124.57	11.0	30.6	20.1	6.31	0.49
	AD 5d	168.87	<b>13.4</b>	32.9	<b>22.0</b>	<b>5.83</b>	<b>0.51</b>
	AD 7d	<i>270.9</i>	<b>15.0</b>	34.9	<b>24.1</b>	<b>5.05</b>	<b>0.56</b>
	AD 9d	<i>351.98</i>	<b>16.8</b>	<b>36.7</b>	<b>25.6</b>	<b>4.95</b>	<b>0.59</b>
AD 20d	<b>1,244.16</b>	<b>21.1</b>	<b>45.1</b>	<b>33.7</b>	<b>2.61</b>	<b>0.71</b>	
Laboratory-aged loose asphalt mix (GB3) with limestone aggregates	AL Fr	4.01	4.8	17.4	8.2	19.76	0.32
	AL Mix	32.55	9.1	24.7	14.7	11.29	0.44
	AL 4h	51.15	8.9	26.4	16.2	9.02	0.42
	AL 2d	106.06	11.5	29.6	19.0	7.77	0.48
	AL 5d	226.78	<b>13.7</b>	32.8	<b>22.1</b>	<b>6.65</b>	<b>0.53</b>
	AL 7d	<i>324.61</i>	<b>14.4</b>	34.6	<b>23.9</b>	<b>5.77</b>	<b>0.57</b>
	AL 9d	<i>372.19</i>	<b>15.7</b>	<b>35.4</b>	<b>24.4</b>	<b>5.92</b>	<b>0.59</b>
AL 20d	<b>1,244.66</b>	<b>21.2</b>	<b>43.7</b>	<b>32.2</b>	<b>3.66</b>	<b>0.67</b>	
Binder from field-aged GB3 mix (Strasbourg)	S B1U	29.21	6.4	23.8	13.5	10.06	0.44
	S B1T	34.41	6.6	23.9	13.8	8.68	0.46
	S B2U	59.65	9.7	26.1	16.1	10.17	0.46
	S B2T	74.04	11.2	27.0	16.9	10.12	0.46
Laboratory-aged binder (Nantes)	N Fr	3.54	6.5	18.1	9.6	16.15	0.28
	N RT	27.63	10.4	24.1	14.9	13.01	0.36
Binder from field-aged GB3 mix (Nantes)	N B2U	15.68	7.9	21.7	12.1	15.15	0.35
	N B2T	13.34	7.3	21.5	11.8	15.74	0.37
	N B3U	157.85	<b>13.2</b>	30.4	20.1	8.70	0.46
	N B3T	<i>181.84</i>	<b>13.2</b>	30.6	20.3	9.00	0.48
Laboratory-aged 10/20 binder from (22)	K1 Fr	107.71	<b>13.2</b>	28.8	18.3	14.16	0.41
	K1 RT	<i>542.25</i>	<b>17.4</b>	<b>35.7</b>	<b>24.67</b>	8.51	<b>0.57</b>
	K1 1P	<b>3,539.70</b>	<b>24.8</b>	<b>49.9</b>	<b>37.4</b>	<b>3.68</b>	<b>0.72</b>

Laboratory-aged 20/30 binder from (22)	K2 Fr	18.08	8.1	23.5	13.4	15.84	0.29
	K2 RT	163.69	<b>13.5</b>	31.4	20.8	9.09	0.47
	K2 1P	<b>1,265.99</b>	<b>21.3</b>	<b>42.9</b>	<b>30.9</b>	<b>5.06</b>	<b>0.64</b>
Laboratory-aged 35/50 binder from (22)	K3 Fr	1.53	6.0	17.9	8.8	24.64	0.17
	K3 RT	6.34	7.6	21.2	11.6	18.53	0.22
	K3 1P	150.08	<b>13.9</b>	31.1	20.5	9.75	0.44
Laboratory-aged 50/70 binder from (22)	K4 Fr	0.54	3.3	16.0	6.9	23.43	0.13
	K4 RT	5.76	6.7	19.4	9.9	19.10	0.25
	K4 1P	77.33	11.5	29.1	18.7	9.52	0.37
Laboratory-aged loose asphalt mix (GB3) with gneiss aggregates	T Fr	27.70	9.1	22.0	12.1	32.93	0.33
	T Mix	104.98	10.5	26.4	16.0	21.63	0.43
	T 4h	320.62	<b>13.2</b>	31.7	20.9	14.18	<b>0.53</b>
	T 2d	<b>674.93</b>	<b>16.0</b>	34.7	<b>23.9</b>	12.78	<b>0.60</b>
	T 5d	<b>1,069.52</b>	<b>17.2</b>	<b>38.2</b>	<b>26.9</b>	10.27	<b>0.63</b>
	T 7d	<b>1,239.50</b>	<b>17.6</b>	<b>39.1</b>	<b>27.8</b>	9.69	<b>0.64</b>
	T 9d	<b>1,719.25</b>	<b>19.1</b>	<b>42.7</b>	<b>31.2</b>	<b>6.23</b>	<b>0.67</b>

The kinetics of all the failure criteria employed in this work was evaluated with the binders AD and AL that were extracted from two different short-term aged loose asphalt mix subjected to long-term aging at 85°C during 2, 5, 7, 9, and 20 days. In (Figure 13), an acceleration in the growth rate of MAI when both binders AD and AL (less accentuated) are close to the limiting value of 0.51 might be the onset of the pseudo-gelation phenomenon in the asphaltene agglomeration system; however, further tests, e.g., Saturate, Aromatic, Resin, and Asphaltene (SARA) fractions as well as GPC, would be necessary to validate it. As for the G-R parameter, this acceleration can also be observed for binder AD.

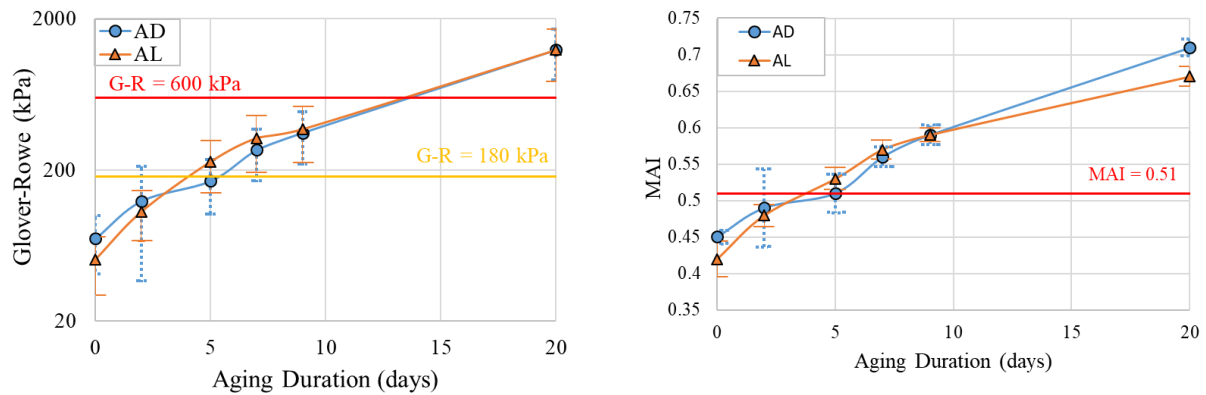


Figure 13 Evolution of G-R (left) and MAI (right) of the binders AD and AL long-term aged in laboratory with their respective error bars (dashed blue line for binder AD and solid orange line for binder AL)

## CONCLUSIONS

Based on the primary findings of this research work, the following conclusions can be drawn:

- The  $\delta$ -method provides valuable insights into the structural changes that may occur within the binder as it ages.
- The Molecular Agglomeration Index (MAI) is proposed to quantify the incidence of asphaltene molecular agglomeration
- The discrepancies in classification between the failure criteria used in this work are due to their particularities.
- The following tentative failure criteria for MAI and  $T_{VET}$  at 0.4 Hz for 35/50 pen grade binders was proposed:

- 1           ○ MAI > 0.51.
- 2           ○  $T_{\text{VET}} > 22^{\circ}\text{C}$  and  $G^*_{\text{VET}} < 7 \text{ MPa}$
- 3       • The acceleration in the growth rate of MAI when binders are close to the limiting value of 0.51
- 4        might be the onset of the pseudo-gelation phenomenon in the asphaltene agglomeration system;
- 5        however, more evidence would be needed to validate it.
- 6
- 7

## 8 **ACKNOWLEDGMENTS**

9 The authors express their acknowledgment to the French National Research Agency (ANR) for the  
10 financial support of the MoveDVDC project (ANR-17-CE22-0014).

## 11 **AUTHOR CONTRIBUTIONS**

12 The authors confirm contribution to the paper as follows: study conception and design: R. Siroma, ML.  
13 Nguyen, and E. Chailleux; data collection: R. Siroma, Y. Hung, A. Nicolai, and L. Ziyani; analysis and  
14 interpretation of results: R. Siroma, ML. Nguyen, P. Hornicy, and T. Lorino; draft manuscript  
15 preparation: R. Siroma, M. Nguyen, and E. Chailleux. All authors reviewed the results and approved the  
16 final version of the manuscript.  
17

## REFERENCES

1. Anderson R, Blankenship P, Zeinali A, King G, Hanson D. Optimal Timing of Preventive Maintenance for Addressing Environmental Aging in Hot-Mix Asphalt Pavements. St. Paul, MN: Minnesota Department of Transportation; 2014 p. 140. Report No.: MN/RC 2014-45.
2. Harvey MO. Optimising Road Maintenance. In: International Transport Forum. Leipzig, Germany; 2012. p. 49.
3. Hunter RN, Self A, Read J. The Shell Bitumen handbook. Sixth edition. Westminster, London: Published for Shell Bitumen by ICE Publishing; 2015. 788 p.
4. Petersen JC. A Review of the Fundamentals of Asphalt Oxidation: Chemical, Physicochemical, Physical Property, and Durability Relationships. Transportation Research Circular. 2009 Oct;(E-C140):78.
5. Lu X, Isacson U. Effect of ageing on bitumen chemistry and rheology. Construction and Building Materials. 2002 Feb;16(1):15–22.
6. Le Guern M, Chailleux E, Farcas F, Dreessen S, Mabilie I. Physico-chemical analysis of five hard bitumens: Identification of chemical species and molecular organization before and after artificial aging. Fuel. 2010 Nov;89(11):3330–9.
7. Mirwald J, Werkovits S, Camargo I, Maschauer D, Hofko B, Grothe H. Investigating bitumen long-term-ageing in the laboratory by spectroscopic analysis of the SARA fractions. Construction and Building Materials. 2020 Oct;258:119577.
8. Petersen JC. Chemical Composition of Asphalt as Related to Asphalt Durability: State of the Art. Transportation Research Record. 1984;(999).
9. Lee S-J, Amirghani SN, Shatanawi K, Kim KW. Short-term aging characterization of asphalt binders using gel permeation chromatography and selected Superpave binder tests. Construction and Building Materials. 2008 Nov;22(11):2220–7.
10. Finn FN, Yapp MT, Coplantz JS, Durrani AZ. Asphalt Properties and Relationship to Pavement Performance: Literature Review. 1990 p. 404.
11. Martin KL, Davison RR, Glover CJ, Bullin JA. Asphalt Aging in Texas Roads and Test Sections. Transportation Research Record. 1990;(1269):9–19.
12. Tuminello WH. Molecular weight and molecular weight distribution from dynamic measurements of polymer melts. Polymer Engineering and Science. 1986 Oct;26(19):1339–47.
13. Wu S. Characterization of polymer molecular weight distribution by transient viscoelasticity: Polytetrafluoroethylenes. Polymer Engineering & Science. 1988;28(8):538–43.

14. Trathnigg B. Handbook of Size Exclusion Chromatography and Related Techniques. Second Edition. (Chromatographic Science Series, Vol. 91.) By Chi-San Wu. Angewandte Chemie International Edition. 2004;43(39):5117–5117.
15. Themeli A, Chailleux E, Farcas F, Chazallon C, Migault B. Molecular weight distribution of asphaltic paving binders from phase-angle measurements. Road Materials and Pavement Design. 2015 May 25;16(sup1):228–44.
16. Zanzotto L, Stastna J, Ho S. Molecular weight distribution of regular asphalts from dynamic material functions. Materials and Structures. 1999 Apr;32(3):224–9.
17. Airey GD. Use of Black Diagrams to Identify Inconsistencies in Rheological Data. Road Materials and Pavement Design. 2002 Jan;3(4):403–24.
18. Lesueur D. The colloidal structure of bitumen: Consequences on the rheology and on the mechanisms of bitumen modification. Advances in Colloid and Interface Science. 2009 Jan;145(1–2):42–82.
19. Siroma RS, Nguyen ML, Hornych P, Lorino T, Chailleux E. Clustering aged bitumens through multivariate statistical analyses using phase angle master curve. Road Materials and Pavement Design. 2021 Jun 1;22(sup1):S51–68.
20. Roche C de la, Ven MV de, Bergh WV den, Gabet T, Dubois V, Porot JG & L. Development of a laboratory bituminous mixtures ageing protocol. Advanced Testing and Characterization of Bituminous Materials, Two Volume Set. 2009.
21. Themeli A, Marsac P, Perez-Martinez M, Krolkral K, Chailleux E. A new method to quantify and evaluate ageing state of asphalt from viscoelastic measurement. In: Proceedings of the international ISAP symposium : from molecules to innovative asphalt pavements. Jackson, Wyoming, USA: International Society for Asphalt Pavement (ISAP); 2016. p. 14.
22. Krolkral K, Haddadi S, Chailleux E. Quantification of asphalt binder ageing from apparent molecular weight distributions using a new approximated analytical approach of the phase angle. Road Materials and Pavement Design. 2018;21(4):1045–60.
23. Di Benedetto H, Gabet T, Grenfell J, Perraton D, Sauzéat C, Bodin D. Mechanical Testing of bituminous Mixtures. In: Advances in Interlaboratory Testing and Evaluation of Bituminous Materials: State-of-the-Art Report of the RILEM Technical Committee 206-ATB. Partl et al. Springer Netherlands; 2013. (RILEM State-of-the-Art Reports).
24. Rowe GM, Sharrock MJ. Cracking of asphalt pavements and the development of specifications with rheological measurements. In: Proceedings of 6th Eurasphalt & Eurobitume Congress. Czech Technical University in Prague; 2016.
25. Chailleux E, Ramond G, Such C, de La Roche C. A mathematical-based master-curve construction method applied to complex modulus of bituminous materials. Road Materials and Pavement Design. 2006 Jan;7(sup1):75–92.

26. Booij HC, Thoone GPJM. Generalization of Kramers-Kronig transforms and some approximations of relations between viscoelastic quantities. *Rheol Acta*. 1982 Jan 1;21(1):15–24.
27. Olard F, Di Benedetto H. General “2S2P1D” Model and Relation Between the Linear Viscoelastic Behaviours of Bituminous Binders and Mixes. *Road Materials and Pavement Design*. 2003 Jan;4(2):185–224.
28. Mullins OC. The Asphaltenes. *Annual Review of Analytical Chemistry*. 2011;4(1):393–418.
29. Rowe GM. Prepared discussion for the AAPT paper by Anderson et al.: Evaluation of the relationship between asphalt binder properties and non-load related cracking. In: *Journal of the Association of Asphalt Paving Technologists* 80. 2011. p. 649–62.
30. Groupe National Bitume. Étude de la fissuration par le haut des bétons bitumineux: suite de l’expérimentation “R.T.F.O.T.” Laboratoire Central des Ponts et Chaussées, editor. Paris, France: Laboratoire central des ponts et chaussées; 1999. 71 p.
31. Ramond G, Such C, Laboratoire central des ponts et chaussées. *Le module complexe des liants bitumineux*. Paris: Laboratoire central des ponts et chaussées; 2003.
32. Widyatmoko D, Elliott R, Heslop M. The Viscous to Elastic Transition Temperature and the In Situ Performance of Bituminous and Asphaltic Materials. *Journal of the Institute of Asphalt Technology*. 2005 May 1;Asphalt Professional No 14:3–7.
33. Khojinian A, Ojum C, Widyatmoko D, D’Angelo G. Identifying Surface Course Deterioration Using Viscous to Elastic Transition (VET) Temperatures. In: *7th Eurasphalt & Eurobitume Congress (E&E Congress 2021)*. Madrid; 2020.
34. Groupe National Bitume. *Pouvoir prédictif de l’essai RTFOT: Compte rendu de synthèse de l’expérimentation*. Paris: Lab.Ctral Ponts&Chaussees; 1992.